

New Mechanics of Knee Joint Injury

Vladimir G. Ivancevic
Defence Science & Technology Organisation, Australia

Abstract

The prediction and prevention of knee joint injury is an important aspect of preventive health science. This paper proposes a new *coupled-loading-rate hypothesis*, which states that the main cause of knee injury is a *Euclidean jolt*, or $SE(3)$ -jolt, an impulsive loading that strikes knee in several coupled degrees-of-freedom simultaneously. Informally, it is a rate-of-change of acceleration in 6-degrees-of-freedom times the body mass, which happens when most of the body mass is on one leg with a semi-flexed knee – and then, caused by some external shock, the knee suddenly ‘jerks’. This can happen in running, skiing, sports games (e.g., soccer, rugby) and various crashes/impacts. To show this formally, based on the previously defined *covariant force law*, we formulate the coupled Newton–Euler dynamics of the knee motions and derive from it the corresponding coupled $SE(3)$ -jolt dynamics. The $SE(3)$ -jolt is the main cause of two forms of discontinuous knee injury: (i) mild rotational disclinations and (ii) severe translational dislocations. Both the knee disclinations and dislocations, as caused by the $SE(3)$ -jolt, are described using the Cosserat multipolar viscoelastic continuum model.

Keywords: knee joint injury, coupled-loading-rate hypothesis, coupled Newton–Euler dynamics, Euclidean jolt dynamics, knee dislocations and disclinations

Contact information:

Dr. Vladimir Ivancevic
Human Systems Integration, Land Operations Division
Defence Science & Technology Organisation, AUSTRALIA
PO Box 1500, 75 Labs, Edinburgh SA 5111
Tel: +61 8 8259 7337, Fax: +61 8 8259 4193
E-mail: Vladimir.Ivancevic@dsto.defence.gov.au

1 Introduction

The knee joint comprises three articulations: (i) a tibio-femoral joint) between the medial and lateral condyles of the femur and tibia (see Figure 1), (ii) patelo-femoral joint between the femur and patella, and (iii) tibio-fibular joint between tibia and fibula. The knee is double condyloid joint, with a dominant flexion/extension. As a synovial joint, the knee has strong fibrous capsule that attaches superiorly to the femur and inferiorly to the articular margin of the tibia. Given its relatively poor bony fit, the knee relies on ligaments for much of its structural stability and integrity. [Whiting and Zernicke 1998].

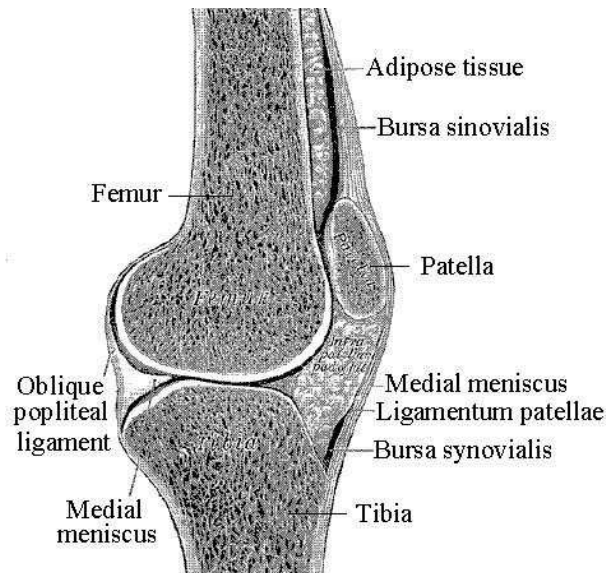


Figure 1: Schematic latero-frontal view of the left knee joint. Although designed to perform mainly flexion/extension (strictly in the sagittal plane) with some restricted medial/lateral rotation in the semi-flexed position, it is clear that the knee joint really has *at least* 6 degrees-of-freedom, including 3 micro-translations. The injury actually occurs when some of these *microscopic* translations become *macroscopic*, which normally happens only after the external jolt.

Knee joint injuries range from mild ligament or meniscus tearing to severe traumatic dislocations (see [Seroyer et al 2008] and references therein) that fall among the most severe form of ligament injury to the lower extremity, associated with a high rate of complications including amputation.

Knee joint injuries are also frequent in sports, especially in ball games. For example, in a recently case-reported complex knee injury in a rugby league player [Shillington et al 2008], resulting in combined rupture of the patellar tendon, anterior cruciate and medial collateral ligaments, with a medial meniscal tear, the video-analysis suggests two points during the tackle when there was the potential for injury: the first occurred when the player was in single leg stance whilst running and received impact to his upper body from three defenders; the second occurred when the player landed on the knee and sustained a valgus and hyper-flexion force under the weight of two defenders. The goal of treatment in this condition is restoration of both the extensor mechanism and knee stability.

Also, the increased number of women participating in sports like soccer has been paralleled by a greater knee injury rate in women compared to men. Among these injuries, those occurring to the anterior cruciate ligament are commonly observed during sidestep cutting maneuvers [Sanna and O'Connor 2008]. In addition, general fatigue appears to correlate with injuries to the passive knee-joint structures during a soccer game.

Besides, the knee is the body part most commonly injured as a consequence of collisions, falls, and overuse occurring from childhood sports. The number of sports-related injuries is increasing because of active participation of children in competitive sports. Children differ from adults in many areas, such as increased rate and ability of healing, higher strength of ligaments compared with growth plates, and continued growth. Growth around the knee can be affected if the growth plates are involved in injuries [Siow et al 2008].

Literature on knee mechanics has been reviewed in [Komistek et al 2005], evaluating various techniques that had been used to determine in ‘vivo loads’ in the human knee joint. Two main techniques that had been used were telemetry – an experimental approach, and mathematical modelling – a theoretical approach. Telemetric analyses had previously been used to determine the ‘in vivo’ loading of the human hip and more recently evaluated in the determination of in vivo knee loads. Mathematical modelling approaches can be categorized in two ways: (i) those that use optimization techniques to solve an indeterminate system, and (ii) those that utilize a reduction method that minimizes the number of unknowns, keeping the system solvable as the number of equations of motion are equal to the number of unknown quantities (for more technical details, see [Komistek et al 2005] and references therein).

The use of a *force-controlled dynamic knee simulator* to quantify the mechanical performance of total knee replacement designs during functional activity was pioneered by [DesJardins et al 2000], in which dynamic *total knee replacement* (TKR) study utilized a 6-degree-of-freedom force-controlled knee simulator to quantify the effect of TKR design alone on TKR mechanics during a simulated walking cycle. Simultaneous prediction of implant kinematics and contact mechanics has been demonstrated using explicit *finite element* (FE) models of the *Instron/Stanmore Knee Joint Simulator, Instron, Canton, MA* [Godest et al 2002, Halloran et al 2005a, Halloran et al 2005b] In these models, kinematic verification was performed by comparing experimental and model-predicted motion for a single implant. Both models were found to produce similar kinematic results. Estimated contact pressure distributions were also closely correlated, as long as significant edge-loading conditions were not present. Recently, an adaptive FE method for pre-clinical wear testing of TKR components was developed in [Knight et al 2007], capable of simulating wear of a polyethylene tibial insert and to compare predicted kinematics, weight loss due to wear, and wear depth contours to results from a force-controlled experimental knee simulator. The displacement-controlled inputs, by accurately matching the experimental tibio-femoral motion, provided an evaluation of the simple wear theory. The force-controlled inputs provided an evaluation of the overall numerical method by simultaneously predicting both kinematics and wear. Proposed international standards for TKR wear simulation have been drafted, yet their methods continue to be debated. The ‘gold standard’ to which all TKR wear testing methodologies should be compared is measured in vivo TKR performance in patients. The study of [DesJardins et al 2007] compared patient TKR kinematics from fluoroscopic analysis and simulator TKR kinematics from force-controlled wear testing to quantify similarities in clinical ranges of motion and contact bearing kinematics and to evaluate the proposed ISO force-controlled Stanmore wear testing methodology.

For human movement purposes, we can say that the safe knee motions (flexion/extension with some medial/lateral rotation in the flexed position) are governed by standard Euler’s rotational dynamics coupled to Newton’s micro-translational dynamics. On the other hand, the unsafe knee events, the main cause of knee injuries, are caused by the knee $SE(3)$ -jolts, the sharp and sudden, “delta”- (forces + torques) combined. These knee $SE(3)$ -jolts do not belong to the standard Newton-Euler dynamics. The only way to monitor them would be to measure “in vivo” the rate of the combined (forces + torques)- rise in the knee joint (see Figure 1).

This paper proposes a new coupled-loading-rate hypothesis, which states that the main cause of knee injury is a Euclidean jolt, or $SE(3)$ -jolt, an impulsive loading that strikes the knee joint in several coupled degrees-of-freedom (DOF) simultaneously. Informally, it is a 6-degree-of-freedom ‘jerk’ (rate-of-change of acceleration) times most-of-the-body mass, which happens when all the body mass is on one leg with a semi-flexed knee – and then, caused by some external shock, the knee ‘jerks’. To show this formally, based on the previously defined *covariant force law*, we formulate the coupled Newton-Euler dynamics of the knee motions and derive from it the corresponding coupled $SE(3)$ -jolt dynamics. The $SE(3)$ -jolt is the main cause of two forms of discontinuous knee injury: (i) mild rotational disclinations and (ii) severe translational dislocations. Both the knee disclinations and dislocations, as caused by the $SE(3)$ -jolt, are described using the Cosserat multipolar viscoelastic continuum model.

While we can intuitively visualize the knee $SE(3)$ -jolt, for the purpose of simulation we use the necessary simplified, decoupled approach (neglecting the 3D torque matrix and its coupling to the 3D force vector). Note that decoupling is a kind of linearization that prevents chaotic behavior, giving an illusion of full predictability. In this decoupled framework of reduced complexity, we define:

The cause of knee dislocations is a linear 3D-jolt vector, the time rate-of-change of a 3D-force

vector (linear jolt = mass \times linear jerk). The cause of knee disclinations is an angular 3-axial jolt, the time rate-of-change of a 3-axial torque (angular jolt = inertia moment \times angular jerk).

This decoupled framework has been implemented in the Human Biodynamics Engine [Ivancevic 2005], a world-class neuro-musculo-skeletal dynamics simulator (with 270 DOFs, the same number of equivalent muscular actuators and two-level neural reflex control), developed by the present author at Defence Science and Technology Organization, Australia. This kinematically validated human motion simulator has been described in a series of papers and books [Ivancevic and Snoswell 2001, Ivancevic and Beagley 2003, Ivancevic 2002, Ivancevic 2004, Ivancevic and Beagley 2005], [Ivancevic and Ivancevic 2006a, Ivancevic and Ivancevic 2006b, Ivancevic and Ivancevic 2006c], [Ivancevic and Ivancevic 2007e, Ivancevic 2006, Ivancevic and Ivancevic 2007a, Ivancevic and Ivancevic 2006, Ivancevic and Ivancevic 2007b, Ivancevic and Ivancevic 2008].

2 The $SE(3)$ -jolt: the main cause of knee injury

In the language of modern biodynamics [Ivancevic 2004, Ivancevic and Ivancevic 2006a], [Ivancevic and Ivancevic 2006b, Ivancevic and Ivancevic 2006c, Ivancevic and Ivancevic 2007d], [Ivancevic and Ivancevic 2007e], the general knee motion is governed by the Euclidean $SE(3)$ -group of 3D motions. Within the knee $SE(3)$ -group we have both $SE(3)$ -kinematics (consisting of the knee $SE(3)$ -velocity and its two time derivatives: $SE(3)$ -acceleration and $SE(3)$ -jerk) and the knee $SE(3)$ -dynamics (consisting of $SE(3)$ -momentum and its two time derivatives: $SE(3)$ -force and $SE(3)$ -jolt), which is the knee kinematics \times the knee mass-inertia distribution.

Informally, the *knee $SE(3)$ -jolt*¹ is a sharp and sudden change in the $SE(3)$ -force acting on the mass-inertia distribution within the knee joint. That is, a ‘delta’-change in a 3D force-vector coupled to a 3D torque-vector, striking the knee. In other words, the knee $SE(3)$ -jolt is a sudden, sharp and discontinuous shock in all 6 coupled dimensions of the knee joint, within the three Cartesian (x, y, z)-translations and the three corresponding Euler angles around the Cartesian axes: roll, pitch and yaw [Ivancevic and Beagley 2003]. If the $SE(3)$ -jolt produces a mild shock to the knee, it causes mild, soft-tissue knee injury. If the $SE(3)$ -jolt produces a hard shock to the knee, it causes severe, hard-tissue knee injury, with the total loss of knee movement.

Therefore, we propose a new *combined loading-rate hypothesis* of the knee injury. This new hypothesis has actually been supported by a number of individual studies, both experimental and numerical, as can be seen from the following brief review.

lit R E V I E W

The knee $SE(3)$ -jolt is rigorously defined in terms of differential geometry [Ivancevic and Ivancevic 2006c, Ivancevic and Ivancevic 2007e]. Briefly, it is the absolute time-derivative of the covariant force 1-form (or, co-vector field) applied to the knee. With this respect, recall that the fundamental law of biomechanics – the so-called *covariant force law* [Ivancevic and Ivancevic 2006b, Ivancevic and Ivancevic 2006c, Ivancevic and Ivancevic 2007e], states:

$$\text{Force co-vector field} = \text{Mass distribution} \times \text{Acceleration vector-field},$$

which is formally written (using the Einstein summation convention, with indices labelling the three local Cartesian translations and the corresponding three local Euler angles):

$$F_\mu = m_{\mu\nu} a^\nu, \quad (\mu, \nu = 1, \dots, 6 = 3 \text{ Cartesian} + 3 \text{ Euler})$$

where F_μ denotes the 6 covariant components of the knee $SE(3)$ -force co-vector field, $m_{\mu\nu}$ represents the 6×6 covariant components of the inertia-metric tensor of the total mass moving in the knee joint, while a^ν corresponds to the 6 contravariant components of the knee $SE(3)$ -acceleration vector-field.

¹The mechanical $SE(3)$ -jolt concept is based on the mathematical concept of higher-order tangency (rigorously defined in terms of jet bundles of the head’s configuration manifold) [Ivancevic and Ivancevic 2006c, Ivancevic and Ivancevic 2007e], as follows: When something hits the human head, or the head hits some external body, we have a collision. This is naturally described by the $SE(3)$ -momentum, which is a nonlinear coupling of 3 linear Newtonian momenta with 3 angular Eulerian momenta. The tangent to the $SE(3)$ -momentum, defined by the (absolute) time derivative, is the $SE(3)$ -force. The second-order tangency is given by the $SE(3)$ -jolt, which is the tangent to the $SE(3)$ -force, also defined by the time derivative.

Now, the covariant (absolute, Bianchi) time-derivative $\frac{D}{dt}(\cdot)$ of the covariant $SE(3)$ -force F_μ defines the corresponding knee $SE(3)$ -jolt co-vector field:

$$\frac{D}{dt}(F_\mu) = m_{\mu\nu} \frac{D}{dt}(a^\nu) = m_{\mu\nu} (\dot{a}^\nu + \Gamma_{\mu\lambda}^\nu a^\mu a^\lambda), \quad (1)$$

where $\frac{D}{dt}(a^\nu)$ denotes the 6 contravariant components of the knee $SE(3)$ -jerk vector-field and overdot $(\dot{\cdot})$ denotes the time derivative. $\Gamma_{\mu\lambda}^\nu$ are the Christoffel's symbols of the Levi-Civita connection for the $SE(3)$ -group, which are zero in case of pure Cartesian translations and nonzero in case of rotations as well as in the full-coupling of translations and rotations.

In the following, we elaborate on the knee $SE(3)$ -jolt concept (using vector and tensor methods) and its biophysical consequences in the form of the knee dislocations and disclinations.

2.1 $SE(3)$ -group of local knee motions

Briefly, the $SE(3)$ -group of knee motions is defined as a semidirect (noncommutative) product of 3D knee rotations and 3D knee micro-translations,

$$SE(3) := SO(3) \triangleright \mathbb{R}^3.$$

Its most important subgroups are the following (see Appendix for technical details):

Subgroup	Definition
$SO(3)$, group of rotations in 3D (a spherical joint)	Set of all proper orthogonal 3×3 – rotational matrices
$SE(2)$, special Euclidean group in 2D (all planar motions)	Set of all 3×3 – matrices: $\begin{bmatrix} \cos \theta & \sin \theta & r_x \\ -\sin \theta & \cos \theta & r_y \\ 0 & 0 & 1 \end{bmatrix}$
$SO(2)$, group of rotations in 2D subgroup of $SE(2)$ -group (a revolute joint)	Set of all proper orthogonal 2×2 – rotational matrices included in $SE(2)$ – group
\mathbb{R}^3 , group of translations in 3D (all spatial displacements)	Euclidean 3D vector space

In other words, the gauge $SE(3)$ -group of knee Euclidean micro-motions contains matrices of the form $\begin{pmatrix} \mathbf{R} & \mathbf{p} \\ 0 & 1 \end{pmatrix}$, where \mathbf{p} is knee 3D micro-translation vector and \mathbf{R} is knee 3D rotation matrix, given by the product $\mathbf{R} = R_\varphi \cdot R_\psi \cdot R_\theta$ of the three Eulerian knee rotations, roll = R_φ , pitch = R_ψ , yaw = R_θ , performed respectively about the x -axis by an angle φ , about the y -axis by an angle ψ , and about the z -axis by an angle θ (see [Ivancevic 2004, Park and Chung 2005, Ivancevic 2006]),

$$R_\varphi = \begin{bmatrix} 1 & 0 & 0 \\ 0 & \cos \varphi & -\sin \varphi \\ 0 & \sin \varphi & \cos \varphi \end{bmatrix}, \quad R_\psi = \begin{bmatrix} \cos \psi & 0 & \sin \psi \\ 0 & 1 & 0 \\ -\sin \psi & 0 & \cos \psi \end{bmatrix}, \quad R_\theta = \begin{bmatrix} \cos \theta & -\sin \theta & 0 \\ \sin \theta & \cos \theta & 0 \\ 0 & 0 & 1 \end{bmatrix}.$$

Therefore, natural knee $SE(3)$ -dynamics is given by the coupling of Newtonian (translational) and Eulerian (rotational) equations of the knee motion.

2.2 Localized knee $SE(3)$ -dynamics

To support our locally-coupled loading-rate hypothesis, we formulate the coupled Newton-Euler dynamics of the knee motions within the $SE(3)$ -group. The forced Newton-Euler equations read in vector (boldface) form

$$\begin{aligned} \text{Newton} & : \quad \dot{\mathbf{p}} \equiv \mathbf{M}\dot{\mathbf{v}} = \mathbf{F} + \mathbf{p} \times \boldsymbol{\omega}, \\ \text{Euler} & : \quad \dot{\boldsymbol{\pi}} \equiv \mathbf{I}\dot{\boldsymbol{\omega}} = \mathbf{T} + \boldsymbol{\pi} \times \boldsymbol{\omega} + \mathbf{p} \times \mathbf{v}, \end{aligned} \quad (2)$$

where \times denotes the vector cross product,²

$$\mathbf{M} \equiv M_{ij} = \text{diag}\{m_1, m_2, m_3\} \quad \text{and} \quad \mathbf{I} \equiv I_{ij} = \text{diag}\{I_1, I_2, I_3\}, \quad (i, j = 1, 2, 3)$$

are the total moving segment's (diagonal) mass and inertia matrices,³ defining the total moving segment mass–inertia distribution, with principal inertia moments given in Cartesian coordinates (x, y, z) by volume integrals

$$I_1 = \iiint \rho(z^2 + y^2) dx dy dz, \quad I_2 = \iiint \rho(x^2 + y^2) dx dy dz, \quad I_3 = \iiint \rho(x^2 + y^2) dx dy dz,$$

dependent on the knee density $\rho = \rho(x, y, z)$,

$$\mathbf{v} \equiv v^i = [v_1, v_2, v_3]^t \quad \text{and} \quad \boldsymbol{\omega} \equiv \omega^i = [\omega_1, \omega_2, \omega_3]^t$$

(where $[\]^t$ denotes the vector transpose) are linear and angular knee–velocity vectors⁴ (that is, column vectors),

$$\mathbf{F} \equiv F_i = [F_1, F_2, F_3] \quad \text{and} \quad \mathbf{T} \equiv T_i = [T_1, T_2, T_3]$$

are gravitational and other external force and torque co-vectors (that is, row vectors) acting on the knee,

$$\begin{aligned} \mathbf{p} &\equiv p_i \equiv \mathbf{M}\mathbf{v} = [p_1, p_2, p_3] = [m_1 v_1, m_2 v_2, m_3 v_3] \quad \text{and} \\ \boldsymbol{\pi} &\equiv \pi_i \equiv \mathbf{I}\boldsymbol{\omega} = [\pi_1, \pi_2, \pi_3] = [I_1 \omega_1, I_2 \omega_2, I_3 \omega_3] \end{aligned}$$

are linear and angular knee–momentum co-vectors.

In tensor form, the forced Newton–Euler equations (2) read

$$\begin{aligned} \dot{p}_i &\equiv M_{ij} \dot{v}^j = F_i + \varepsilon_{ik}^j p_j \omega^k, \quad (i, j, k = 1, 2, 3) \\ \dot{\pi}_i &\equiv I_{ij} \dot{\omega}^j = T_i + \varepsilon_{ik}^j \pi_j \omega^k + \varepsilon_{ik}^j p_j v^k, \end{aligned}$$

where the permutation symbol ε_{ik}^j is defined as

$$\varepsilon_{ik}^j = \begin{cases} +1 & \text{if } (i, j, k) \text{ is } (1, 2, 3), (3, 1, 2) \text{ or } (2, 3, 1), \\ -1 & \text{if } (i, j, k) \text{ is } (3, 2, 1), (1, 3, 2) \text{ or } (2, 1, 3), \\ 0 & \text{otherwise: } i = j \text{ or } j = k \text{ or } k = i. \end{cases}$$

In scalar form, the forced Newton–Euler equations (2) expand as

$$\begin{aligned} \text{Newton} &: \begin{cases} \dot{p}_1 = F_1 - m_3 v_3 \omega_2 + m_2 v_2 \omega_3 \\ \dot{p}_2 = F_2 + m_3 v_3 \omega_1 - m_1 v_1 \omega_3 \\ \dot{p}_3 = F_3 - m_2 v_2 \omega_1 + m_1 v_1 \omega_2 \end{cases}, \\ \text{Euler} &: \begin{cases} \dot{\pi}_1 = T_1 + (m_2 - m_3) v_2 v_3 + (I_2 - I_3) \omega_2 \omega_3 \\ \dot{\pi}_2 = T_2 + (m_3 - m_1) v_1 v_3 + (I_3 - I_1) \omega_1 \omega_3 \\ \dot{\pi}_3 = T_3 + (m_1 - m_2) v_1 v_2 + (I_1 - I_2) \omega_1 \omega_2 \end{cases}, \end{aligned} \quad (3)$$

showing the moving segment's mass and inertia couplings.

Equations (2)–(3) can be derived from the translational + rotational kinetic energy of the moving segment⁵

$$E_k = \frac{1}{2} \mathbf{v}^t \mathbf{M} \mathbf{v} + \frac{1}{2} \boldsymbol{\omega}^t \mathbf{I} \boldsymbol{\omega}, \quad (4)$$

²Recall that the cross product $\mathbf{u} \times \mathbf{v}$ of two vectors \mathbf{u} and \mathbf{v} equals $\mathbf{u} \times \mathbf{v} = uv \sin \theta \mathbf{n}$, where θ is the angle between \mathbf{u} and \mathbf{v} , while \mathbf{n} is a unit vector perpendicular to the plane of \mathbf{u} and \mathbf{v} such that \mathbf{u} and \mathbf{v} form a right-handed system.

³In reality, mass and inertia matrices (\mathbf{M}, \mathbf{I}) are not diagonal but rather full 3×3 positive–definite symmetric matrices with coupled mass– and inertia–products. Even more realistic, fully–coupled mass–inertia properties of a moving segment are defined by the single non-diagonal 6×6 positive–definite symmetric mass–inertia matrix $\mathcal{M}_{SE(3)}$, the so-called material metric tensor of the $SE(3)$ –group, which has all nonzero mass–inertia coupling products. However, for simplicity, in this paper we shall consider only the simple case of two separate diagonal 3×3 matrices (\mathbf{M}, \mathbf{I}).

⁴In reality, $\boldsymbol{\omega}$ is a 3×3 *attitude matrix* (see Appendix). However, for simplicity, we will stick to the (mostly) symmetrical translation–rotation vector form.

⁵In a fully–coupled Newton–Euler knee dynamics, instead of equation (4) we would have moving segment's kinetic energy defined by the inner product:

$$E_k = \frac{1}{2} [\mathbf{p} \boldsymbol{\pi} | \mathcal{M}_{SE(3)} | \mathbf{p} \boldsymbol{\pi}].$$

or, in tensor form

$$E = \frac{1}{2}M_{ij}\dot{v}^i\dot{v}^j + \frac{1}{2}I_{ij}\dot{\omega}^i\dot{\omega}^j.$$

For this we use the *Kirchhoff–Lagrangian equations* (see, e.g., [Lamb 1932, Leonard 1997], or the original work of Kirchhoff in German)

$$\begin{aligned} \frac{d}{dt}\partial_{\mathbf{v}}E_k &= \partial_{\mathbf{v}}E_k \times \boldsymbol{\omega} + \mathbf{F}, \\ \frac{d}{dt}\partial_{\boldsymbol{\omega}}E_k &= \partial_{\boldsymbol{\omega}}E_k \times \boldsymbol{\omega} + \partial_{\mathbf{v}}E_k \times \mathbf{v} + \mathbf{T}, \end{aligned} \quad (5)$$

where $\partial_{\mathbf{v}}E_k = \frac{\partial E_k}{\partial \mathbf{v}}$, $\partial_{\boldsymbol{\omega}}E_k = \frac{\partial E_k}{\partial \boldsymbol{\omega}}$; in tensor form these equations read

$$\begin{aligned} \frac{d}{dt}\partial_{v^i}E &= \varepsilon_{ik}^j (\partial_{v^j}E) \omega^k + F_i, \\ \frac{d}{dt}\partial_{\omega^i}E &= \varepsilon_{ik}^j (\partial_{\omega^j}E) \omega^k + \varepsilon_{ik}^j (\partial_{v^j}E) v^k + T_i. \end{aligned}$$

Using (4)–(5), linear and angular knee–momentum co–vectors are defined as

$$\mathbf{p} = \partial_{\mathbf{v}}E_k, \quad \boldsymbol{\pi} = \partial_{\boldsymbol{\omega}}E_k,$$

or, in tensor form

$$p_i = \partial_{v^i}E, \quad \pi_i = \partial_{\omega^i}E,$$

with their corresponding time derivatives, in vector form

$$\dot{\mathbf{p}} = \frac{d}{dt}\mathbf{p} = \frac{d}{dt}\partial_{\mathbf{v}}E, \quad \dot{\boldsymbol{\pi}} = \frac{d}{dt}\boldsymbol{\pi} = \frac{d}{dt}\partial_{\boldsymbol{\omega}}E,$$

or, in tensor form

$$\dot{p}_i = \frac{d}{dt}p_i = \frac{d}{dt}\partial_{v^i}E, \quad \dot{\pi}_i = \frac{d}{dt}\pi_i = \frac{d}{dt}\partial_{\omega^i}E,$$

or, in scalar form

$$\dot{\mathbf{p}} = [\dot{p}_1, \dot{p}_2, \dot{p}_3] = [m_1\dot{v}_1, m_2\dot{v}_2, m_3\dot{v}_3], \quad \dot{\boldsymbol{\pi}} = [\dot{\pi}_1, \dot{\pi}_2, \dot{\pi}_3] = [I_1\dot{\omega}_1, I_2\dot{\omega}_2, I_3\dot{\omega}_3].$$

While healthy knee $SE(3)$ –dynamics is given by the coupled Newton–Euler micro–dynamics, the knee injury is actually caused by the sharp and discontinuous change in this natural $SE(3)$ micro–dynamics, in the form of the $SE(3)$ –jolt, causing discontinuous knee deformations, both translational dislocations and rotational disclinations.

2.3 Knee injury dynamics: the $SE(3)$ –jolt

The $SE(3)$ –jolt, the actual cause of the knee injury (in the form of the plastic deformations), is defined as a coupled Newton+Euler jolt; in (co)vector form the $SE(3)$ –jolt reads⁶

$$SE(3) - \text{jolt} : \begin{cases} \text{Newton jolt} : \dot{\mathbf{F}} = \ddot{\mathbf{p}} - \dot{\mathbf{p}} \times \boldsymbol{\omega} - \mathbf{p} \times \dot{\boldsymbol{\omega}}, \\ \text{Euler jolt} : \dot{\mathbf{T}} = \ddot{\boldsymbol{\pi}} - \dot{\boldsymbol{\pi}} \times \boldsymbol{\omega} - \boldsymbol{\pi} \times \dot{\boldsymbol{\omega}} - \dot{\mathbf{p}} \times \mathbf{v} - \mathbf{p} \times \dot{\mathbf{v}}, \end{cases}$$

where the linear and angular jolt co–vectors are

$$\dot{\mathbf{F}} \equiv \mathbf{M}\ddot{\mathbf{v}} = [\dot{F}_1, \dot{F}_2, \dot{F}_3], \quad \dot{\mathbf{T}} \equiv \mathbf{I}\ddot{\boldsymbol{\omega}} = [\dot{T}_1, \dot{T}_2, \dot{T}_3],$$

where

$$\ddot{\mathbf{v}} = [\ddot{v}_1, \ddot{v}_2, \ddot{v}_3]^t, \quad \ddot{\boldsymbol{\omega}} = [\ddot{\omega}_1, \ddot{\omega}_2, \ddot{\omega}_3]^t,$$

are linear and angular jerk vectors.

⁶Note that the derivative of the cross–product of two vectors follows the standard calculus product–rule: $\frac{d}{dt}(\mathbf{u} \times \mathbf{v}) = \dot{\mathbf{u}} \times \mathbf{v} + \mathbf{u} \times \dot{\mathbf{v}}$.

In tensor form, the $SE(3)$ -jolt reads⁷

$$\begin{aligned}\dot{F}_i &= \ddot{p}_i - \varepsilon_{ik}^j \dot{p}_j \omega^k - \varepsilon_{ik}^j p_j \dot{\omega}^k, & (i, j, k = 1, 2, 3) \\ \dot{T}_i &= \ddot{\pi}_i - \varepsilon_{ik}^j \dot{\pi}_j \omega^k - \varepsilon_{ik}^j \pi_j \dot{\omega}^k - \varepsilon_{ik}^j \dot{p}_j v^k - \varepsilon_{ik}^j p_j \dot{v}^k,\end{aligned}$$

in which the linear and angular jolt covectors are defined as

$$\begin{aligned}\dot{\mathbf{F}} &\equiv \dot{F}_i = \mathbf{M}\dot{\mathbf{v}} \equiv M_{ij}\dot{v}^j = [\dot{F}_1, \dot{F}_2, \dot{F}_3], \\ \dot{\mathbf{T}} &\equiv \dot{T}_i = \mathbf{I}\dot{\omega} \equiv I_{ij}\dot{\omega}^j = [\dot{T}_1, \dot{T}_2, \dot{T}_3],\end{aligned}$$

where $\dot{\mathbf{v}} = \ddot{v}^i$, and $\dot{\omega} = \ddot{\omega}^i$ are linear and angular jerk vectors.

In scalar form, the $SE(3)$ -jolt expands as

$$\begin{aligned}\text{Newton jolt} &: \begin{cases} \dot{F}_1 = \ddot{p}_1 - m_2\omega_3\dot{v}_2 + m_3(\omega_2\dot{v}_3 + v_3\dot{\omega}_2) - m_2v_2\dot{\omega}_3, \\ \dot{F}_2 = \ddot{p}_2 + m_1\omega_3\dot{v}_1 - m_3\omega_1\dot{v}_3 - m_3v_3\dot{\omega}_1 + m_1v_1\dot{\omega}_3, \\ \dot{F}_3 = \ddot{p}_3 - m_1\omega_2\dot{v}_1 + m_2\omega_1\dot{v}_2 - v_2\dot{\omega}_1 - m_1v_1\dot{\omega}_2, \end{cases} \\ \text{Euler jolt} &: \begin{cases} \dot{T}_1 = \ddot{\pi}_1 - (m_2 - m_3)(v_3\dot{v}_2 + v_2\dot{v}_3) - (I_2 - I_3)(\omega_3\dot{\omega}_2 + \omega_2\dot{\omega}_3), \\ \dot{T}_2 = \ddot{\pi}_2 + (m_1 - m_3)(v_3\dot{v}_1 + v_1\dot{v}_3) + (I_1 - I_3)(\omega_3\dot{\omega}_1 + \omega_1\dot{\omega}_3), \\ \dot{T}_3 = \ddot{\pi}_3 - (m_1 - m_2)(v_2\dot{v}_1 + v_1\dot{v}_2) - (I_1 - I_2)(\omega_2\dot{\omega}_1 + \omega_1\dot{\omega}_2). \end{cases}\end{aligned}$$

We remark here that the linear and angular momenta (\mathbf{p}, π), forces (\mathbf{F}, \mathbf{T}) and jolts ($\dot{\mathbf{F}}, \dot{\mathbf{T}}$) are co-vectors (row vectors), while the linear and angular velocities (\mathbf{v}, ω), accelerations ($\dot{\mathbf{v}}, \dot{\omega}$) and jerks ($\ddot{\mathbf{v}}, \ddot{\omega}$) are vectors (column vectors). This bio-physically means that the ‘jerk’ vector should not be confused with the ‘jolt’ co-vector. For example, the ‘jerk’ means shaking the head’s own mass–inertia matrices (mainly in the atlanto–occipital and atlanto–axial joints), while the ‘jolt’ means actually hitting the head with some external mass–inertia matrices included in the ‘hitting’ $SE(3)$ -jolt, or hitting some external static/massive body with the head (e.g., the ground – gravitational effect, or the wall – inertial effect). Consequently, the mass-less ‘jerk’ vector represents a (translational+rotational) *non-collision effect* that can cause only soft knee injuries, while the inertial ‘jolt’ co-vector represents a (translational+rotational) *collision effect* that can cause hard knee injuries.

For example, while driving a car, the $SE(3)$ -jerk of the head–neck system happens every time the driver brakes abruptly. On the other hand, the $SE(3)$ -jolt means actual impact to the head. Similarly, the whiplash–jerk, caused by rear–end car collisions, is like a soft version of the high pitch–jolt caused by the boxing ‘upper-cut’. Also, violently shaking the head left–right in the transverse plane is like a soft version of the high yaw–jolt caused by the boxing ‘cross-cut’.

2.4 Knee disclinations and dislocations caused by the $SE(3)$ -jolt

For mild knee injury, the best injury predictor is considered to be the product of localized knee strain and strain rate, which is the standard isotropic viscoelastic continuum concept. To improve this standard concept, in this subsection, we consider the knee joint as a 3D anisotropic multipolar *Cosserat viscoelastic continuum* [Cosserat and Cosserat 1898, Cosserat and Cosserat 1909, Eringen 2002], exhibiting coupled–stress–strain elastic properties. This non-standard continuum model is suitable for analyzing plastic (irreversible) deformations and fracture mechanics [Bilby and Eshelby 1968] in multi-layered materials with microstructure (in which slips and bending of layers introduces additional degrees of freedom, non-existent in the standard continuum models; see [Mindlin 1965, Lakes 1985] for physical characteristics and [Yang and Lakes 1981, Yang and Lakes 1982], [Park and Lakes 1986] for biomechanical applications).

The $SE(3)$ -jolt ($\mathbf{F}, \dot{\mathbf{T}}$) causes two types of localized knee discontinuous deformations:

1. The Newton jolt $\dot{\mathbf{F}}$ can cause severe micro-translational *dislocations*, or discontinuities in the Cosserat translations;

⁷In this paragraph the overdots actually denote the absolute Bianchi (covariant) time-derivative (1), so that the jolts retain the proper covector character, which would be lost if ordinary time derivatives are used. However, for the sake of simplicity and wider readability, we stick to the same overdot notation.

2. The Euler jolt $\dot{\mathbf{T}}$ can cause mild micro-rotational *disclinations*, or discontinuities in the Cosserat rotations.

For general treatment on dislocations and disclinations related to asymmetric discontinuous deformations in multipolar materials, see, e.g., [Jian and Xiao-ling 1995, Yang et al 2001].

To precisely define the knee dislocations and disclinations, caused by the $SE(3)$ -jolt $(\dot{\mathbf{F}}, \dot{\mathbf{T}})$, we first define the coordinate co-frame, i.e., the set of basis 1-forms $\{dx^i\}$, given in local coordinates $x^i = (x^1, x^2, x^3) = (x, y, z)$, attached to the moving segment's center-of-mass. Then, in the coordinate co-frame $\{dx^i\}$ we introduce the following set of the knee plastic-deformation-related $SE(3)$ -based differential p -forms (see [Ivancevic and Ivancevic 2006c, Ivancevic and Ivancevic 2007e]):

the *dislocation current* 1-form, $\mathbf{J} = J_i dx^i$;

the *dislocation density* 2-form, $\alpha = \frac{1}{2}\alpha_{ij} dx^i \wedge dx^j$;

the *disclination current* 2-form, $\mathbf{S} = \frac{1}{2}S_{ij} dx^i \wedge dx^j$; and

the *disclination density* 3-form, $\mathbf{Q} = \frac{1}{3!}Q_{ijk} dx^i \wedge dx^j \wedge dx^k$,

where \wedge denotes the exterior wedge-product. According to Edelen [Edelen 1980, Kadic and Edelen 1983], these four $SE(3)$ -based differential forms satisfy the following set of continuity equations:

$$\dot{\alpha} = -\mathbf{d}\mathbf{J} - \mathbf{S}, \quad (6)$$

$$\dot{\mathbf{Q}} = -\mathbf{d}\mathbf{S}, \quad (7)$$

$$\mathbf{d}\alpha = \mathbf{Q}, \quad (8)$$

$$\mathbf{d}\mathbf{Q} = \mathbf{0}, \quad (9)$$

where \mathbf{d} denotes the exterior derivative.

In components, the simplest, fourth equation (9), representing the *Bianchi identity*, can be rewritten as

$$\mathbf{d}\mathbf{Q} = \partial_l Q_{[ijk]} dx^l \wedge dx^i \wedge dx^j \wedge dx^k = 0,$$

where $\partial_i \equiv \partial/\partial x^i$, while $\theta_{[ij\dots]}$ denotes the skew-symmetric part of $\theta_{ij\dots}$.

Similarly, the third equation (8) in components reads

$$\begin{aligned} \frac{1}{3!}Q_{ijk} dx^i \wedge dx^j \wedge dx^k &= \partial_k \alpha_{[ij]} dx^k \wedge dx^i \wedge dx^j, \quad \text{or} \\ Q_{ijk} &= -6\partial_k \alpha_{[ij]}. \end{aligned}$$

The second equation (7) in components reads

$$\begin{aligned} \frac{1}{3!}\dot{Q}_{ijk} dx^i \wedge dx^j \wedge dx^k &= -\partial_k S_{[ij]} dx^k \wedge dx^i \wedge dx^j, \quad \text{or} \\ \dot{Q}_{ijk} &= 6\partial_k S_{[ij]}. \end{aligned}$$

Finally, the first equation (6) in components reads

$$\begin{aligned} \frac{1}{2}\dot{\alpha}_{ij} dx^i \wedge dx^j &= (\partial_j J_i - \frac{1}{2}S_{ij}) dx^i \wedge dx^j, \quad \text{or} \\ \dot{\alpha}_{ij} &= 2\partial_j J_i - S_{ij}. \end{aligned}$$

In words, we have:

- The 2-form equation (6) defines the time derivative $\dot{\alpha} = \frac{1}{2}\dot{\alpha}_{ij} dx^i \wedge dx^j$ of the dislocation density α as the (negative) sum of the disclination current \mathbf{S} and the curl of the dislocation current \mathbf{J} .
- The 3-form equation (7) states that the time derivative $\dot{\mathbf{Q}} = \frac{1}{3!}\dot{Q}_{ijk} dx^i \wedge dx^j \wedge dx^k$ of the disclination density \mathbf{Q} is the (negative) divergence of the disclination current \mathbf{S} .
- The 3-form equation (8) defines the disclination density \mathbf{Q} as the divergence of the dislocation density α , that is, \mathbf{Q} is the *exact* 3-form.
- The Bianchi identity (9) follows from equation (8) by *Poincaré lemma* [Ivancevic and Ivancevic 2006c, Ivancevic and Ivancevic 2007e] and states that the disclination density \mathbf{Q} is conserved quantity, that is, \mathbf{Q} is the *closed* 3-form. Also, every 4-form in 3D space is zero.

From these equations, we can conclude that the knee dislocations and disclinations are mutually coupled by the underlying $SE(3)$ -group, which means that we cannot separately analyze translational and rotational knee injuries — a fact which *is not* supported by the literature.

3 Conclusion

Based on the previously developed covariant force law, in this paper we have formulated a new coupled loading–rate hypothesis for the knee injury, which states that the main cause of the knee injury is an external $SE(3)$ –jolt, an impulsive loading striking the knee in several degrees-of-freedom, both rotational and translational, combined. To demonstrate this, we have developed the vector Newton–Euler mechanics on the Euclidean $SE(3)$ –group of the knee micro-motions. In this way, we have precisely defined the concept of the $SE(3)$ –jolt, which is a cause of two kinds of rapid knee discontinuous deformations: (i) mild rotational disclinations, and (ii) severe translational dislocations. Based on the presented model, we argue that we cannot separately analyze localized knee rotations from translations, as they are in reality coupled. To prevent knee injuries we need to develop the *external $SE(3)$ –jolt awareness*.

4 Appendix: The $SE(3)$ –group

Special Euclidean group $SE(3) := SO(3) \triangleright \mathbb{R}^3$, (the semidirect product of the group of rotations with the corresponding group of translations), is the Lie group consisting of isometries of the Euclidean 3D space \mathbb{R}^3 .

An element of $SE(3)$ is a pair (A, a) where $A \in SO(3)$ and $a \in \mathbb{R}^3$. The action of $SE(3)$ on \mathbb{R}^3 is the rotation A followed by translation by the vector a and has the expression

$$(A, a) \cdot x = Ax + a.$$

The Lie algebra of the Euclidean group $SE(3)$ is $\mathfrak{se}(3) = \mathbb{R}^3 \times \mathbb{R}^3$ with the Lie bracket

$$[(\xi, u), (\eta, v)] = (\xi \times \eta, \xi \times v - \eta \times u). \quad (10)$$

Using homogeneous coordinates, we can represent $SE(3)$ as follows,

$$SE(3) = \left\{ \begin{pmatrix} R & p \\ 0 & 1 \end{pmatrix} \in GL(4, \mathbb{R}) : R \in SO(3), p \in \mathbb{R}^3 \right\},$$

with the action on \mathbb{R}^3 given by the usual matrix–vector product when we identify \mathbb{R}^3 with the section $\mathbb{R}^3 \times \{1\} \subset \mathbb{R}^4$. In particular, given

$$g = \begin{pmatrix} R & p \\ 0 & 1 \end{pmatrix} \in SE(3),$$

and $q \in \mathbb{R}^3$, we have

$$g \cdot q = Rq + p,$$

or as a matrix–vector product,

$$\begin{pmatrix} R & p \\ 0 & 1 \end{pmatrix} \begin{pmatrix} q \\ 1 \end{pmatrix} = \begin{pmatrix} Rq + p \\ 1 \end{pmatrix}.$$

The Lie algebra of $SE(3)$, denoted $\mathfrak{se}(3)$, is given by

$$\mathfrak{se}(3) = \left\{ \begin{pmatrix} \omega & v \\ 0 & 0 \end{pmatrix} \in M_4(\mathbb{R}) : \omega \in \mathfrak{so}(3), v \in \mathbb{R}^3 \right\},$$

where the attitude (or, angular velocity) matrix $\omega : \mathbb{R}^3 \rightarrow \mathfrak{so}(3)$ is given by

$$\omega = \begin{pmatrix} 0 & -\omega_z & \omega_y \\ \omega_z & 0 & -\omega_x \\ -\omega_y & \omega_x & 0 \end{pmatrix}.$$

The *exponential map*, $\exp : \mathfrak{se}(3) \rightarrow SE(3)$, is given by

$$\exp \begin{pmatrix} \omega & v \\ 0 & 0 \end{pmatrix} = \begin{pmatrix} \exp(\omega) & Av \\ 0 & 1 \end{pmatrix},$$

where

$$A = I + \frac{1 - \cos \|\omega\|}{\|\omega\|^2} \omega + \frac{\|\omega\| - \sin \|\omega\|}{\|\omega\|^3} \omega^2,$$

and $\exp(\omega)$ is given by the *Rodriguez' formula*,

$$\exp(\omega) = I + \frac{\sin \|\omega\|}{\|\omega\|} \omega + \frac{1 - \cos \|\omega\|}{\|\omega\|^2} \omega^2.$$

References

- [Seroyer et al 2008] Seroyer, S.T., Musahl, V., Harner, C.D. Management of the acute knee dislocation: The Pittsburgh experience. *Injury (Elsevier)*, **39**(7), 710–718, (2008)
- [Shillington et al 2008] Shillington, M., Logan, M., Myers, P. A complex knee injury in a rugby league player Combined rupture of the patellar tendon, anterior cruciate and medial collateral ligaments, with a medial meniscal tear. *Injury Extra (Elsevier)*, in press, available online PubMed, (2008)
- [Sanna and O'Connor 2008] Sanna, G., O'Connor, K.M. Fatigue-related changes in stance leg mechanics during sidestep cutting maneuvers. *Clin. Biomech.* (in press), available online PubMed, (2008)
- [Siow et al 2008] Siow, H.M., Cameron, D.B., Ganley, T.J. Acute Knee Injuries in Skeletally Immature Athletes. *Phys. Med. Rehab.* **19**(2), 319–345, (2008)
- [Komistek et al 2005] Komistek, R.D., Kane, T.R., Mahfouz, M., Ochoa, J.A., Dennis, D.A. Knee mechanics: a review of past and present techniques to determine in vivo loads. *J. Biomech.* **38**(2), 215–228, (2005)
- [DesJardins et al 2000] DesJardins, J.D., Walker, P.S., Haider, H., Perry, J. The use of a force-controlled dynamic knee simulator to quantify the mechanical performance of total knee replacement designs during functional activity. *J. Biomech.* **33**, 1231–1242, (2000)
- [Godest et al 2002] Godest, A.C., Beaugonin, M., Haug, E., Taylor, M., Gregson, P.J. Simulation of a knee joint replacement during a gait cycle using explicit finite element analysis, *J. Biomech.* **35**(2), 267-275, (2002)
- [Halloran et al 2005a] Halloran, J.P., Easley, S.K., Petrella, A.J., Rullkoetter, P. Comparison of deformable and elastic foundation finite element simulations for predicting knee replacement mechanics. *J. Biomech. Eng.* **127**, 813818, (2005)
- [Halloran et al 2005b] Halloran, J.P., Petrella, A.J., Rullkoetter, P. Explicit finite element modeling of TKR mechanics. *J. Biomech.* **38**, 323-331, (2005)
- [Knight et al 2007] Knight, L.A., Pal, S., Coleman, J.C., Bronson, F., Haider, H., Levine, D.L., Taylor, M., Rullkoetter, P.J. Comparison of long-term numerical and experimental total knee replacement wear during simulated gait loading. *J. Biomech.* **40**, 1550–1558, (2007)
- [DesJardins et al 2007] DesJardins, J.D., Banks, S.A., Benson, L.C., Pace, T., LaBerge, M. A direct comparison of patient and force-controlled simulator total knee replacement kinematics. *J. Biomech.* **40**, 3458-3466, (2007)
- [Whiting and Zernicke 1998] Whiting, W.C., Zernicke, R.F. *Biomechanics of Musculoskeletal Injury.* Human Kinetics, Champaign, IL, (1998).

- [Ivancevic and Snoswell 2001] Ivancevic, V., Snoswell, M. Fuzzy-Stochastic Functor Machine for General Humanoid-Robot Dynamics. *IEEE Trans. Sys. Man Cyber. B*, **31**(3), 319-330, (2001).
- [Ivancevic 2002] Ivancevic, V. Generalized Hamiltonian Biodynamics and Topology Invariants of Humanoid Robots. *Int. J. Math. & Math. Sci.* **31**(9), 555-565, (2002).
- [Ivancevic 2004] Ivancevic, V. Symplectic Rotational Geometry in Human Biomechanics. *SIAM Rev.* **46**(3), 455-474, (2004).
- [Ivancevic 2005] Ivancevic, V. Human Biodynamics Engine – Full Spine Simulator. Australian Defence Excellence in Science & Technology Award 2005 for Physiological Modelling, Adelaide, (2005).
- [Ivancevic and Beagley 2005] Ivancevic, V., Beagley, N. Brain-like functor control machine for general humanoid biodynamics. *Int. J. Math. & Math. Sci.* **11**, 1759-1779, (2005).
- [Ivancevic 2006] Ivancevic, V., Lie-Lagrangian model for realistic human biodynamics. *Int. J. Hum. Rob.* **3**(2), 205-218, (2006).
- [Ivancevic and Ivancevic 2006a] Ivancevic, V., Ivancevic, T., Natural Biodynamics. World Scientific, Singapore, (2006).
- [Ivancevic and Ivancevic 2006b] Ivancevic, V., Ivancevic, T., Human-Like Biomechanics. Springer, Dordrecht, (2006).
- [Ivancevic and Ivancevic 2006c] Ivancevic, V., Ivancevic, T., Geometrical Dynamics of Complex systems: A Unified Modelling Approach to Physics, Control, Biomechanics, Neurodynamics and Psycho-Socio-Economical Dynamics. Springer, Dordrecht, (2006).
- [Ivancevic and Ivancevic 2006] Ivancevic, V., Ivancevic, T., High-Dimensional Chaotic and Attractor Systems. Springer, Berlin, (2006).
- [Ivancevic and Ivancevic 2007a] Ivancevic, V., Ivancevic, T., Neuro-Fuzzy Associative Machinery for Comprehensive Brain and Cognition Modelling. Springer, Berlin, (2007).
- [Ivancevic and Ivancevic 2007b] Ivancevic, V., Ivancevic, T., Computational Mind: A Complex Dynamics Perspective. Springer, Berlin, (2007).
- [Ivancevic and Ivancevic 2007d] Ivancevic, V., Ivancevic, T., Complex Dynamics: Advanced System Dynamics in Complex Variables. Springer, Dordrecht, (2007).
- [Ivancevic and Ivancevic 2007e] Ivancevic, V., Ivancevic, T., Applied Differential Geometry: A Modern Introduction. World Scientific, Singapore, (2007).
- [Ivancevic and Ivancevic 2008] Ivancevic, V., Ivancevic, T., Complex Nonlinearity: Chaos, Phase Transitions, Topology Change and Path Integrals. Springer, Berlin, (2008).
- [Ivancevic and Beagley 2003] Ivancevic, V., Beagley, N., Mathematical twist reveals the agony of back pain. *New Scientist*, 9 Aug. (2003).
- [Bilby and Eshelby 1968] Bilby, B.A., Eshelby, J.D., Dislocation and the Theory of Fracture. In: *Fracture, An Advanced Treatise*, Liebowitz, H., (ed). I, Microscopic and Macroscopic Fundamentals, Academic Press, New York and London, 99-182, (1968).

- [Cosserat and Cosserat 1898] Cosserat, E., Cosserat, F., Sur les equations de la theorie de l'elasticite. C.R. Acad. Sci. Paris, **126**, 1089-1091, (1898).
- [Cosserat and Cosserat 1909] Cosserat, E., Cosserat, F., Theorie des Corps Deformables. Hermann et Fils, Paris, (1909).
- [Edelen 1980] Edelen, D.G.B., A four-dimensional formulation of defect dynamics and some of its consequences, Int. J. Engng. Sci. **18**, 1095, (1980).
- [Eringen 2002] Eringen, A.C., Nonlocal Continuum Field Theories. Springer, New York, (2002).
- [Jian and Xiao-ling 1995] Jian, G., Xiao-ling, L., A Physical theory of asymmetric plasticity. Appl. Math. Mech. (Springer), 16(5), 493-506, (1995).
- [Kadic and Edelen 1983] Kadic, A., Edelen, D.G.B., A Gauge theory of Dislocations and Disclinations. Springer, New York, (1983).
- [Lakes 1985] Lakes, R.S., A pathological situation in micropolar elasticity. J. Appl. Mech. **52**, 234-235, (1985).
- [Lamb 1932] Lamb, H., Hydrodynamics (6th ed). Dover, New York, (1932).
- [Leonard 1997] Leonard, N.E., Stability of a bottom-heavy underwater vehicle. Automatica, **33**(3), 331-346, (1997).
- [Mindlin 1965] Mindlin, R.D., Stress functions for a Cosserat continuum. Int. J. Solids Struct. **1**, 265-271, (1965).
- [Park and Chung 2005] Park, J., Chung, W.-K. Geometric Integration on Euclidean Group With Application to Articulated Multibody Systems. IEEE Trans. Rob. **21**(5), 850-863, (2005).
- [Park and Lakes 1986] Park, H.C., Lakes, R.S., Cosserat micromechanics of human bone: strain redistribution by a hydration-sensitive constituent. J. Biomech. **19**, 385-397, (1986).
- [Yang and Lakes 1981] Yang, J.F.C., Lakes, R.S., Transient study of couple stress in compact bone: torsion, J. Biomech. Eng. **103**, 275-279, (1981).
- [Yang and Lakes 1982] Yang, J.F.C., Lakes, R.S., Experimental study of micropolar and couple-stress elasticity in bone in bending. J. Biomech. **15**, 91-98, (1982).
- [Yang et al 2001] Yang, W., Tang, J-C., Ing, Y-S., Ma, C-C., Transient dislocation emission from a crack tip. J. Mech. Phys. Solids, **49**(10), 2431-2453, (2001).